



“Gheorghe Asachi” Technical University of Iasi, Romania



APPLYING TRIGONOMETRIC LEVELLING FOR MONITORING THE VERTICAL DEFORMATIONS OF ENGINEERING STRUCTURES

Constantin Chirilă*, Raluca Maria Albu-Budusanu

“Gheorghe Asachi” Technical University of Iasi, Faculty of Hydrotechnical Engineering, Geodesy and Environmental Engineering, Department of Terrestrial Measurements and Cadastre, 65 Dimitrie Mangeron Blvd, 700050 Iasi, Romania

Abstract

Among the usual geodetic methods of vertical deformations measuring of structures and natural objects, geometrical levelling is one of the most accurate, but also requires compliance to specific conditions of slope and terrain accessibility. Where geometrical levelling is difficult or impossible to apply, the trigonometric levelling can be a viable practical solution, if there are followed a series of procedures to improve the accuracy of the final results.

For the case of classical geodetic measurements, where the network geometry has an important role, a high accuracy solution for the height differences has to ensure the mean square errors as small as possible in the vertical direction of the chosen coordinate system. In this situation, the whole monitoring network will be aligned in one vertical plane, so determining checkpoints height will result by a forward intersection in vertical plane.

The functional model of the adjustment method will include only zenith angles measurements, but horizontal distances are used to determine the coordinates of landmarks in a rectangular vertical system. Thus, by the imposed geometry of the network, the new points' coordinates will have a weaker component determined on the alignment direction of the benchmarks and a precise component determined on the height direction. In terms of graphical expression, after network adjustment by least squares method, the error ellipses will result in a very elongated geometric conformation, which are flattened in the interested direction of the height. The case study consisted in applying method to an area of a pedestrian bridge, in which was simulated the vertical deformations by means of control points of adjustable height. Two cycles were performed for monitoring vertical deformations compared with the results of the geometric levelling measurements. The results showed that for short distances, the differences obtained for control points' height between the two methods were in the range $[2.1 \div 5.7 \text{ mm}]$ in both cycles of measurements. Height differences calculated between the two successive cycles of all the control points between the two methods were within the range of accuracy $[0.8 \div 1.9 \text{ mm}]$. For long distances, this procedure of trigonometric levelling could provide improved results for height differences, in order to reduce the influence of zenith angles errors due to vertical atmospheric refraction.

Key words: error ellipse, forward intersection, height difference, trigonometric levelling, vertical deformation

Received: May, 2018; Revised final: October, 2018; Accepted: October, 2018; Published in final edited form: September, 2019

1. Introduction

Among the geodetic methods for monitoring the vertical deformations, one of the most precise and widely used method is the geometrical levelling method (Nistor, 1993). Under special circumstances, when the route has an accentuated slope or discontinuities that prevent the development of a

levelling line, the solution is to use trigonometric levelling (Ceylan et al., 2005).

The trigonometric levelling method has a restricted accuracy caused by the length of the sight line. As the sight length grows the measured height difference is influenced by the vertical atmospheric refraction (Moldoveanu, 2002). Taking into consideration the fact that, usually, monitoring engineering structures falls within the range of small

* Author to whom all correspondence should be addressed: e-mail: constantin.chirila@tuiasi.ro, ralucaalbu@gmail.com

distances of several hundred meters, the careful and appropriate application of trigonometric levelling can approximate the geometric levelling accuracy (Nistor, 1993). For the trigonometric levelling with station spacing at 200 – 300 m, measured by a precise total station, it can be neglected the influence of vertical refraction errors, as well as the effect of vertical deflections (Torge, 2001).

If the motorized trigonometric levelling technique is applied, in which the vehicles are a part of the measuring system, the results obtained lead to a standard deviation of about ± 0.5 mm/km, results that are similar to the motorized geometric levelling technique (Becker and Lithen, 1986; Becker et al., 1988; Becker, 2002; Chrzanowski, 1989; Chirilă et al., 2015).

Usually, it can be stated that high-order results can be obtained in trigonometric levelling by following specific procedures, regarding the angular and distance accuracy of instrument, special targets, redundancies of measurements, sight distances and specific corrections (Ghilani and Wolf, 2012). Using the advantages of trigonometric levelling as efficiently where the terrain is rugged, with frequent changes in elevation or where there are special engineering structures to be observed only remotely due to the high security or physical inaccessibility, it is possible to perform a vertical deformations monitoring with high precision.

For this purpose, a monitoring network will be designed, which will include at least 4 fixed stations and an optimal number of control marks located on the structure of the construction to be tracked. Basically, we have to determine the height of the new landmarks by using a forward intersection in the vertical plane from the reference points with known coordinates. As there are redundancies of measurements, the network's adjustment will be accomplished by using the least-squares method corrections (Ghilani and Wolf, 2006). Such an approach provides a complete picture on the precision of the results obtained, with the advantage of highlighting small errors resulting in the vertical direction due to the special configuration of the network's geometry (Teunissen, 2006 a, b, 2009).

The method was tested on a pedestrian bridge in the Iasi area over a distance of less than 100 m. The simulation of subsidence between two measurement cycles was accomplished through a controlled displacement of the checkpoints, the comparison between the obtained results being in relation to the measurements resulted from geometrical levelling.

2. Material and methods

The method consists of using a number of at least 4 station points of known height (A, B, C, D) resulting in some distance measurements and then, for each cycle, in some zenith angles measurements toward the control points (1, 2, ... , n) whose heights are required to be determined (Fig. 1).

By applying the angle forward intersection method based on the least squares principle to a new point, his height will result in a coordinates system situated on a vertical plane.

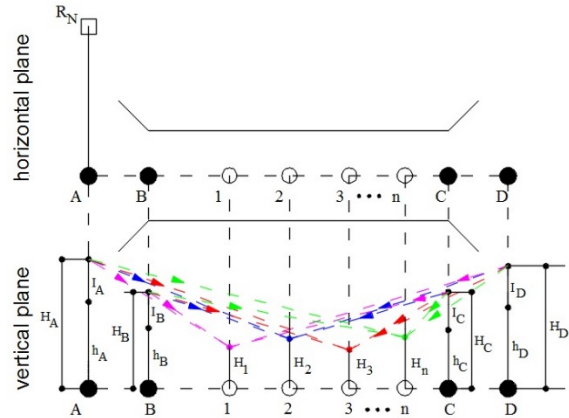


Fig. 1. The principle of the forward intersection in vertical plane method

This is possible as for every new point there will be 4 determination sight lines, therefore a number of redundancies which is necessary in order to apply the minimum principle (Fig. 2).

The natural origin of the coordinate system (*d*, *H*) is considered to be the point A, with:

- The *d* axis, located horizontally in the direction of the alignment joining the 4 reference points (A, B, C, D);
- The *H* axis, located vertically in the station point, A.

The origin of the axis system will be translated to the left (in the opposite direction of the B, C, D points) with a rounded value (example: $d_A = 100$ m).

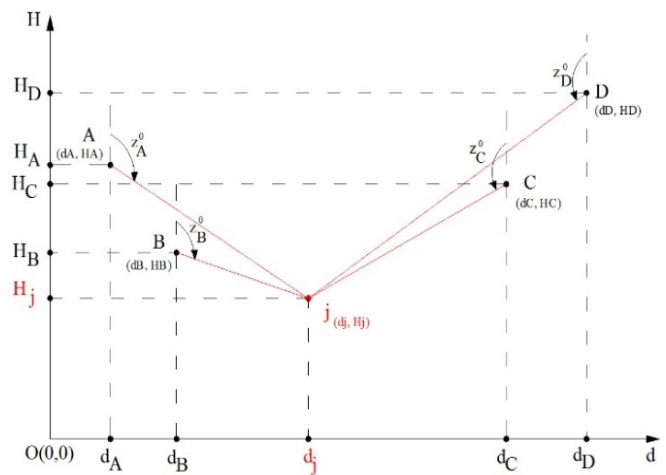


Fig. 2. Forward intersection in vertical plane (*d*, *H*)

Therefore, the (*d*, *H*) coordinates of point A in the translated system will be (Eqs. 1-2):

$$d_A = 100 \text{ m}; \tag{1}$$

$$H_A = h_A + I_A. \tag{2}$$

For the H_A coordinate we will take into consideration adding the height of instrument (I_A) to the height of point (h_A). For all the other reference points, the d coordinate will be obtained by adding the horizontal distance from point A to the given point (B, C, D) to the d coordinate of point A (d_A) (Eqs. 3-5):

$$d_B = d_A + D_{AB}; \quad (3)$$

$$d_C = d_A + D_{AC}; \quad (4)$$

$$d_D = d_A + D_{AD}. \quad (5)$$

The H coordinate of the reference points (B, C, D) will be the result of adding the height of instrument to the height of the considered point, similarly to the previous case (Eqs. 6-8):

$$H_B = h_B + I_B; \quad (6)$$

$$H_C = h_C + I_C; \quad (7)$$

$$H_D = h_D + I_D. \quad (8)$$

In order to determine the initial approximations of the (d , H) control points coordinates we can use the known formulas from the angle forward intersection in horizontal plane (Onose, 2004) by making the necessary adaptations for the vertical plane:

- the θ orientations of the reference points directions located on the left of the control point will be replaced with the measured zenith angles (z°);

- the θ orientations of the reference points directions located on the right of the control point will be replaced with ($400^g - z^\circ$), where z° represents the zenith angle measured to the new point.

For example, according to Fig. 2, we can deduct the following formulas we can use in order to calculate the (d , H) coordinates for the new point 2, obtained by combining the A and D known points (Eqs. 9-10):

$$d_2 = \frac{d_A \tan(z_A^\circ) - d_D \tan(400^g - z_D^\circ) - H_A + H_D}{\tan(z_A^\circ) - \tan(400^g - z_D^\circ)}; \quad (9)$$

$$H_2 = H_A + (d_2 - d_A) \tan(z_A^\circ) = H_D + (d_2 - d_D) \tan(400^g - z_D^\circ). \quad (10)$$

The initial approximations of the new points coordinates will be further introduce in the rigorous processing based on the principle of least squares by using the indirect measurements method. In the case of the functional model, the most important stage is the forming of the observation equations system. The total number of the observation equations will be equal to the number of sight lines performed from every station point to the corresponding control points. Therefore, the adjustment model will be repeatedly applied to every new point. Every observation equation will be written distinctly, depending on the

left or right position of direction towards the new point.

- **Case I** (the reference point is to the left of the new point) – example A-1 (Fig. 3)

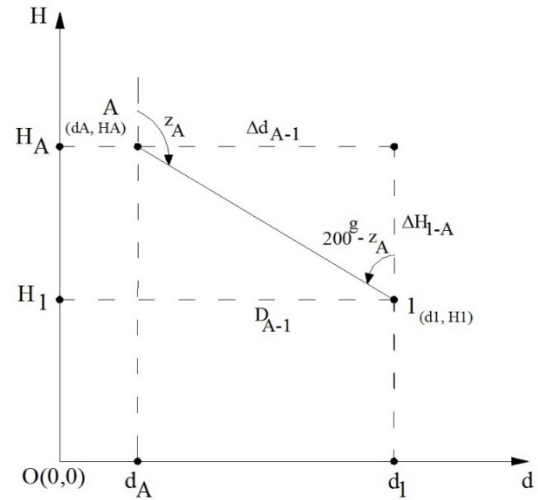


Fig. 3. New point determination (Case 1)

According to Fig. 3, we can see that (Eq. 11):

$$\tan(200^g - z_A) = \frac{\Delta d_{A1}}{\Delta H_{A1}} \Rightarrow \tan(z_A) = \frac{\Delta d_{A1}}{\Delta H_{A1}} \Rightarrow z_A = \arctan \frac{d_1 - d_A}{H_1 - H_A} + 200^g. \quad (11)$$

For linearizing the z_A function, we will apply a first-order Taylor series expansion around point 1 of initial approximated coordinates (d_1^o, H_1^o) (Eqs. 12-14):

$$z_A = z_A^* + \left(\frac{\partial z_A}{\partial d_1} \right)_0 dd_1 + \left(\frac{\partial z_A}{\partial H_1} \right)_0 dH_1, \quad (12)$$

$$\text{where } z_A^* = \arctan \frac{d_1^o - d_A}{H_1^o - H_A} + 200^g. \quad (13)$$

From the equality (Eq. 14):

$$z_A = z_A^* + dz_A \Rightarrow dz_A = \left(\frac{\partial z_A}{\partial d_1} \right)_0 dd_1 + \left(\frac{\partial z_A}{\partial H_1} \right)_0 dH_1, \quad (14)$$

where dd_1 , dH_1 are the unknown parameters and the partial derivatives of the z_A function with respect to d_1 , H_1 are evaluated at the initial approximated values (d_1^o, H_1^o) (Eqs. 15-16):

$$\left(\frac{\partial z_A}{\partial d_1} \right)_0 = \frac{1}{1 + \left(\frac{\Delta d_{A1}^o}{\Delta H_{A1}^o} \right)^2} \frac{\Delta H_{A1}^o}{(\Delta H_{A1}^o)^2} = \frac{\Delta H_{A1}^o}{(\Delta H_{A1}^o)^2 + (\Delta d_{A1}^o)^2}; \quad (15)$$

$$\left(\frac{\partial z_A}{\partial H_1}\right)_0 = \frac{1}{1 + \left(\frac{\Delta d_{A1}^o}{\Delta H_{A1}^o}\right)^2} \frac{-\Delta d_{A1}^o}{(\Delta H_{A1}^o)^2} = \frac{\Delta d_{1A}^o}{(\Delta H_{A1}^o)^2 + (\Delta d_{A1}^o)^2} \tag{16}$$

In order to express the partial derivatives from the above relations as a variation of seconds per meter, we need to introduce the notations of following coefficients (Eqs. 17-18):

$$a_1 \left[\frac{cc}{m} \right] = \rho^{cc} \frac{H_1^o - H_A}{(H_1^o - H_A)^2 + (d_1^o - d_A)^2}; \tag{17}$$

$$a_2 \left[\frac{cc}{m} \right] = \rho^{cc} \frac{d_A - d_1^o}{(H_1^o - H_A)^2 + (d_1^o - d_A)^2}. \tag{18}$$

Therefore, the equation for the variation of the zenith angle depending on the variation of the rectangular coordinates (d, H) will be (Eq. 19):

$$dz_A^{cc} = a_1 dd_1 + a_2 dH_1. \tag{19}$$

The fact that there are more observations regarding the zenith angle starting from the point A to the new point 1 will result in a mean angle (z_A^o) computed as the average of the “ n ” individual measurements (Eq. 20):

$$z_A^o = \frac{1}{n} \sum_{i=1}^n z_{Ai}^o. \tag{20}$$

We will add the following correction (v_{A-1}) to the initial approximation (z_A^o) in order to calculate the adjusted zenith angle (z_A) (Eq. 21):

$$z_A = z_A^o + v_{A1}. \tag{21}$$

Therefore (Eq. 22):

$$v_{A1} = z_A - z_A^o = (z_A^* + dz_A) - z_A^o = dz_A + (z_A^* - z_A^o). \tag{22}$$

In order to express the correction in seconds, we will write (Eq. 23):

$$v_{A1}^{cc} = d_{z_A}^{cc} + l_{A1}^{cc} = a_1 dd_1 + a_2 dH_1 + l_{A1}^{cc}, \tag{23}$$

where $l_{A1}^{cc} = (z_A^* - z_A^o)^{cc}$.

- **Case 2** (the reference point is to the right of the new point) – example C-1 (Fig. 4)

According to Fig. 4, we can see that (Eq. 24):

$$\tan(200^g - z_C) = \frac{\Delta d_{1C}}{\Delta H_{1C}} \Rightarrow \tan(z_C) = \frac{\Delta d_{C1}}{\Delta H_{1C}} \Rightarrow$$

$$z_C = \arctan \frac{d_1 - d_C}{H_C - H_1} + 200^g. \tag{24}$$

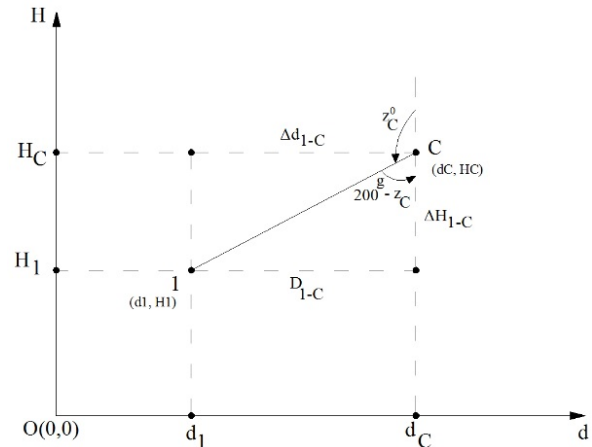


Fig. 4. New point determination (Case 2)

For linearizing the z_C function, we will apply a first-order Taylor series expansion around point 1 of initial approximated coordinates (d_1^o, H_1^o) (Eqs. 25-26):

$$z_C = z_C^* + \left(\frac{\partial z_C}{\partial d_1}\right)_0 dd_1 + \left(\frac{\partial z_C}{\partial H_1}\right)_0 dH_1, \tag{25}$$

$$\text{where } z_C^* = \arctan \frac{d_1^o - d_C}{H_C^o - H_1^o} + 200^g. \tag{26}$$

From the equality (Eq. 27):

$$z_C = z_C^* + dz_C \Rightarrow dz_C = \left(\frac{\partial z_C}{\partial d_1}\right)_0 dd_1 + \left(\frac{\partial z_C}{\partial H_1}\right)_0 dH_1, \tag{27}$$

where (Eqs. 28-29):

$$\left(\frac{\partial z_C}{\partial d_1}\right)_0 = \frac{1}{1 + \left(\frac{\Delta d_{C1}^o}{\Delta H_{1C}^o}\right)^2} \frac{\Delta H_{1C}^o}{(\Delta H_{1C}^o)^2} = \frac{\Delta H_{1C}^o}{(\Delta H_{1C}^o)^2 + (\Delta d_{C1}^o)^2}; \tag{28}$$

$$\left(\frac{\partial z_C}{\partial H_1}\right)_0 = \frac{1}{1 + \left(\frac{\Delta d_{C1}^o}{\Delta H_{1C}^o}\right)^2} \frac{-\Delta d_{C1}^o}{(\Delta H_{1C}^o)^2} = \frac{\Delta d_{C1}^o}{(\Delta H_{1C}^o)^2 + (\Delta d_{C1}^o)^2}. \tag{29}$$

In order to express dz_C in seconds, we need to introduce the following coefficients notations (Eqs. 30-31):

$$c_1 \left[\frac{cc}{m} \right] = \rho^{cc} \frac{H_C - H_1^o}{(H_C - H_1^o)^2 + (d_1^o - d_C)^2}; \tag{30}$$

$$c_2 \left[\frac{cc}{m} \right] = \rho^{cc} \frac{d_1^o - d_c}{(H_c - H_1^o)^2 + (d_1^o - d_c)^2}. \quad (31)$$

The equation for the variation of the zenith angle depending on the variation of the rectangular coordinates (d, H) will be (Eq. 32):

$$dz_c^{cc} = c_1 dd_1 + c_2 dH_1. \quad (32)$$

The fact that there are more observations regarding the zenith angle starting from the point C to the new point 1 will result in a mean angle (z_C^o) computed as the average of the “ n ” individual measurements (Eq. 33):

$$z_C^o = \frac{1}{n} \sum_{i=1}^n z_{Ci}^o. \quad (33)$$

We will add the following correction ($v_{C,1}$) to the initial approximation (z_C^o) in order to calculate the adjusted zenith angle (z_C) (Eq. 34):

$$z_C = z_C^o + v_{C,1}. \quad (34)$$

Hence, the first case follows (Eq. 35):

$$v_{C,1} = z_C - z_C^o = (z_C^* + dz_C) - z_C^o = dz_C + (z_C^* - z_C^o). \quad (35)$$

In order to express the correction in seconds, we will obtain (Eqs. 36-37):

$$v_{C,1}^{cc} = d_{z_C}^{cc} + l_{C,1}^{cc} = c_1 dd_1 + c_2 dH_1 + l_{C,1}^{cc}, \quad (36)$$

where

$$l_{C,1}^{cc} = (z_C^* - z_C^o)^{cc}. \quad (37)$$

Following that, the observation equations will be grouped in matrix form according to the standard algorithm (Chirilă, 2014) (Eqs. 38-39):

$$A_{r,2} X_{2,1} + L_{r,1} = V_{r,1} \quad (38)$$

where $W_{r,r}$ is the weight matrix; r represents the number of sight lines from the reference points ($r = 4$), (Eq. 40):

$$A_{r,2} = \begin{bmatrix} a_1 & a_2 \\ b_1 & b_2 \\ c_1 & c_2 \\ d_1 & d_2 \end{bmatrix}; X_{2,1} = \begin{bmatrix} dd_1 \\ dH_1 \end{bmatrix}; L_{r,1} = \begin{bmatrix} l_{A,1} \\ l_{B,1} \\ l_{C,1} \\ l_{D,1} \end{bmatrix}; V_{r,1} = \begin{bmatrix} v_{A,1} \\ v_{B,1} \\ v_{C,1} \\ v_{D,1} \end{bmatrix}; \quad (39)$$

$$W_{r,r} = \begin{bmatrix} w_{A,1} & 0 & 0 & 0 \\ 0 & w_{B,1} & 0 & 0 \\ 0 & 0 & w_{C,1} & 0 \\ 0 & 0 & 0 & w_{D,1} \end{bmatrix}. \quad (40)$$

The weight of each equation is inversely proportional to the variance of the measured zenith angle (Eq. 41):

$$w_{A,1} = \frac{1}{s(z_{A,1}^o)^2}; \dots; w_{D,1} = \frac{1}{s(z_{D,1}^o)^2}. \quad (41)$$

The transition to the normal equations system will be made based on the minimum condition [wv] → min, resulting in the following matrix form (Eqs. 42-43):

$$N_{2,2} X_{2,1} + T_{2,1} = O_{2,1} \quad (42)$$

where

$$N_{2,2} = (A_{2,r})^T W_{r,r} A_{r,2}, T_{2,1} = (A_{2,r})^T W_{r,r} L_{r,1}. \quad (43)$$

The unknown parameters can be obtained by solving the normal equations system through the inverse of the normal matrix (Eqs. 44-45):

$$X_{2,1} = - (N_{2,2})^{-1} T_{2,1} = - Q_{2,2} T_{2,1} \quad (44)$$

$$\text{where } Q_{2,2} = - (N_{2,2})^{-1}. \quad (45)$$

The adjusted values resulted at the end of the processing will be (Eqs. 46-47):

- the zenith angles:

$$z_i = z_i^o + v_{z_i}, \quad i=\{A, B, C, D\} \quad (46)$$

- the rectangular coordinates (d, H) of the new point:

$$d_1 = d_1^o + dd_1; \quad H_1 = H_1^o + dH_1. \quad (47)$$

After the final check of the adjustment where the adjusted zenith angles must be equal to the ones resulted from the adjusted coordinates of the new point and the known ones of the reference points, we must go through the stages of evaluating the precision of the results (Eqs. 48-50):

- the reference standard deviation of unit weight:

$$s_0 = \pm \sqrt{\frac{V^T W V}{r - 2}}, \quad (48)$$

- the standard deviations for the weighted observations (zenith angles):

$$s_{z_i} = \pm \frac{s_0}{\sqrt{w_i}}; \tag{49}$$

- the standard deviations of the adjusted coordinates:

$$s_d = \pm s_0 \sqrt{Q_{dd}}; \quad s_H = \pm s_0 \sqrt{Q_{HH}}, \tag{50}$$

where Q_{dd} and Q_{HH} are diagonal elements from the covariance matrix (Q_{11} ; Q_{22}), corresponding to the unknown parameters (d , H).

In this case, the error of particular interest is the standard deviation of the adjusted height. Due to the special geometrical configuration of measuring the zenith angles, this error will be very small while on the horizontal direction, which is of little interest, the error will be rather large.

3. Results and discussion

The studied objective is the “Trancu” pedestrian bridge in Iasi, “Splai Bahlui” area (Fig. 5).



Fig. 5. Studied objective: “Trancu” pedestrian bridge

Concerning the monitoring of the vertical deformations of the studied objective, the control marks located on the construction have been lowered in a controlled manner in order to simulate a potential subsidence during two successive measurement cycles. In order to apply the trigonometric levelling method, the distances and zenith angles measurements have been performed with a LEICA TCR 407 total station. In order to make a comparison, measurements of the height differences through geometric levelling have been executed with a LEICA Sprinter 100M level.

Within the trigonometric levelling network, the A , B , C and D benchmarks will be considered fixed points, of known height; therefore we must determine the heights by using the precise method of geometric levelling. For this purpose, a geometric levelling traverse has been executed, based on the benchmark of known height R_N ($H_{RN} = 100$ m) thus obtaining the height of the A , B , C and D benchmarks (Fig. 6).

As a preliminary stage, necessary to the rigorous adjustment of the trigonometric levelling network, the horizontal distances from A to the B , C , D benchmarks and 1 , 2 , 3 control points have been determined in order to calculate their initial

approximated coordinates in the vertical rectangular system (Fig. 7).

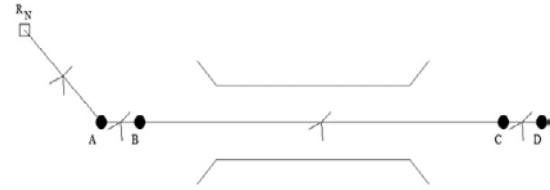


Fig. 6. Geometric levelling traverse



Fig. 7. Trigonometric levelling network

The projected trigonometric levelling network is made up of 4 benchmarks with known coordinates (d , H) and 3 new control marks whose heights are going to be determined by angular measurements to both observation cycles. For every new point of the network, it is presented the measured zenith angles from the fixed points (Fig. 8).

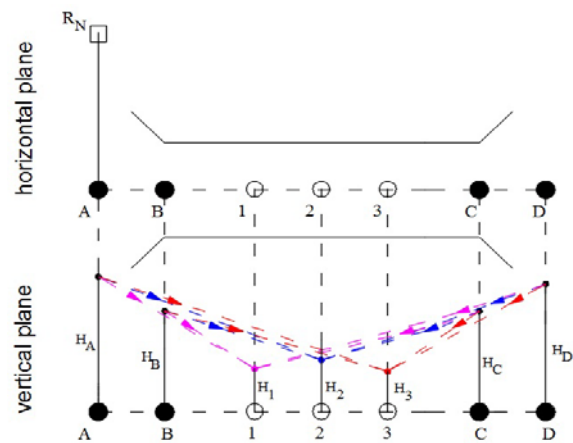


Fig. 8. The sight lines of the trigonometric levelling network

Following the above algorithm [paragraph 2], we obtained the adjusted coordinates (d , H) for the control points and the mean square errors associated to every measurement cycle.

In order to evaluate the precision of the results obtained using the trigonometric levelling method, only the standard deviations of the adjusted heights of

new points, in every measurement cycle, will be selected for analysis (Table 1).

Table 1. The standard deviations of the adjusted heights of new points

New landmark	Standard deviations of the adjusted heights s_H [mm]	
	cycle 0	cycle 1
1	0.5	0.1
2	0.5	0.5
3	0.2	0.2

It is noticeable that the range of values in which the standard deviation of the adjusted height (s_H) falls is [0.1 – 0.5 mm].

For a proper comparison of the adjusted network’s global precision for every new point it is presented the reference standard deviation of unit weight (s_0) obtained in both measurement cycles (Table 2).

Table 2. The evaluation of adjusted network’s global precision

New landmark	Reference standard deviation of unit weight (s_0)	
	cycle 0	cycle 1
1	2.010766	1.235451
2	2.394738	1.847033
3	1.948683	1.265024

For the second landmark, the measurements from the first cycle were affected by blunders. Following the data analysis, a large error of the D station was identified and therefore the D point has been removed from the adjustment in order to improve the determination precision of the new landmark (no. 2).

In order to compare the obtained results with the ones of the geometric levelling measurements we had to calculate the differences between the heights obtained by trigonometric levelling and the ones obtained by geometric levelling for both measurement cycles (Table 3).

Table 3. Height differences between trigonometric levelling and geometric levelling

New landmark	Height differences between trigonometric levelling and geometric levelling [mm]	
	cycle 0	cycle 1
1	3.9	-2.1
2	5.7	4.8
3	3.7	5.0

Another edifying comparison can be observed between the height differences resulted from the two measurement cycles both for trigonometric levelling and geometric levelling (Table 4).

We can observe that the differences in value between the discussed methods (*trigonometric levelling and geometric levelling*) fall within the range [0.9-1.9 mm]. Approaching the final results between

the two methods is due in this case to the fact that the height differences between the two measurement cycles remove a series of errors that occur within the trigonometric levelling method, especially in height instrument measurement. [There is no change of height instrument between successive cycles of observation].

Table 4. Height differences between the measurement cycles

New landmark	Height differences between the measurement cycles [mm]		Differences [mm] (TL)-(GL)
	Trigonometric levelling (TL)	Geometric levelling (GL)	
1	6.0	7.9	-1.9
2	6.1	5.2	0.9
3	6.6	7.8	-1.3

4. Conclusions

This paper proposes a method of applying the trigonometric levelling on a vertical deformations monitoring network. The method should lead to a better precision of determining the control points’ heights. The functional model in adjustment computations using the least squares principle contains only zenith angles measurements, the whole processing being adapted to a rectangular coordinate system in vertical plane.

The principle of determining the heights of the new landmarks is based on the calculation of the forward intersection in vertical plane from at least 4 reference points disposed on a single alignment.

Due to the special geometric configuration of the sight lines’ intersection in the new points with obtuse angles, this will lead to the error ellipses with extremely flat conformation that highlight smaller errors on the vertical direction and larger errors on the horizontal direction, which are not of interest.

Following the evaluation of the precision resulted from applying the method to the study case, we can observe that the standard deviation of the adjusted height of the new points did not exceed 0.5 mm. By comparing the heights determined by trigonometric levelling with the ones of the geometric levelling, the differences were up to 5.7 mm. By comparing the height differences resulted from the measurement cycles, through trigonometric levelling and geometric levelling, maximum value did not exceed 1.9 mm.

In conclusion, we can state that the method is viable and can be successfully applied to short distances when, for objective reasons, we cannot use the geometric levelling. An example is also a local geodetic network designed for the 3D calibration test-field, to obtain a homogeneous and unitary precision of all three components of spatial positioning (Oniga et al., 2013, 2018).

For further research, it would be useful to study the same kind of network on longer distances, noting the effect of vertical atmospheric refraction on the determination of the zenith angle.

When measuring the height of instrument, it is recommended to use a careful approach and if there are no changes of instrument position between the measurement cycles, we could remove it by calculating the height differences between successive measurements. Not least, using a total station with higher angular accuracy can lead to better results and less value for the standard deviation of the adjusted height.

References

- Becker J.M., Lithen T., (1986), *Motorized Trigonometric Levelling (MTL) and Motorized XYZ Technique (MXYZ) in Sweden*, FIG Congress'86, Toronto, Canada, On line at: <https://www.lantmateriet.se/globalassets/kartor-och-geografisk-information/gps-och-geodetisk-matning/rapporter/1986-8.pdf>
- Becker J.M., Lithen T., Nordquist A., (1988), *Experience of Motorized Trigonometric Levelling (MTL) - a Comparison with other Techniques*, Gavle, Sweden, On line at: <https://www.lantmateriet.se/globalassets/kartor-och-geografisk-information/gps-och-geodetisk-matning/rapporter/1988-23.pdf>
- Becker J.M., (2002), *Levelling over the Oresund Bridge at the Millimetre Level*, FIG Congress 2002, USA, https://www.lantmateriet.se/globalassets/kartor-och-geografisk-information/gps-och-geodetisk-matning/publikationer/fig_congress_2002_levelling_over_the_oresund_bridge_at_the_millimetre_level_by_jmb_dk-sweden.pdf
- Ceylan A., Inal C., Sanlioglu I., (2005), *Modern Height Determination Techniques and Comparison of Accuracies*, FIG Working Week 2005 and GSDI-8, Cairo, Egypt, On line at: https://www.fig.net/resources/proceedings/fig_proceedings/cairo/papers/ts_33/ts33_05_ceylan_et_al.pdf
- Chirilă C., (2014), *Mathematical Geodesy. Guide of Practical Works and Project*, Tehnopress Publishing House, Iași, Romania.
- Chirilă C., Onu C., Tulan A.C., (2015), Study on the efficiency of using motorized levelling in vertical geodetic networks, *Journal of Geodesy, Cartography and Cadastre*, **2**, 34-49.
- Chrzanowski A., (1989), Implementation of trigonometric height traversing in geodetic levelling of high precision, Technical Report No. 142, Department of Surveying Engineering, University of New Brunswick, Canada, On line at: <http://www2.unb.ca/gge/Pubs/TR142.pdf>
- Ghilani D.C., Wolf P.R., (2006), *Adjustment Computations. Spatial Data Analysis*, Fourth edition, John Wiley & Sons, Inc, Hoboken, New Jersey, U.S.A.
- Ghilani D.C., Wolf P.R., (2012), *Elementary Surveying. An Introduction to Geomatics*, 13th Edition, Pearson Education, Inc., Upper Saddle River, New Jersey, U.S.A.
- Moldoveanu C., (2002), *Geodesy. Concepts of Physical and Ellipsoidal Geodesy, Positioning*, Matrix Rom Publishing House, Bucharest, Romania.
- Nistor G., (1993), *Geodesy Applied to the Construction Study*, "Gheorghe Asachi" Publishing House, Iași, Romania.
- Oniga E., Diac M., (2013), Metric and non-metric cameras calibration for the improvement of real-time monitoring process results, *Environmental Engineering and Management Journal*, **12**, 719-726.
- Oniga E., Pfeifer N., Loghin A., (2018), 3D calibration test-field for digital cameras mounted on Unmanned Aerial Systems (UAS), *Remote Sensing*, **10**, <https://doi.org/10.3390/rs10122017>.
- Onose D., (2004), *Topography*, Matrix Rom Publishing House, București, Romania.
- Teunissen P.J.G., (2006a), *Network Quality Control*, VSSD Publishing House, Delft, The Netherlands.
- Teunissen P.J.G., (2006b), *Testing Theory*, VSSD Publishing House, Delft, The Netherlands.
- Teunissen P.J.G., (2009), *Adjustment Theory*, VSSD Publishing House, Delft, The Netherlands.
- Torge W., (2001), *Geodesy*, 3rd Edition, Berlin, Germany.